Measurement 149 (2020) 107041

Contents lists available at ScienceDirect

Measurement

journal homepage: www.elsevier.com/locate/measurement

A new test method and system for the circumferential deformation of cylindrical standard specimens in geotechnical mechanics and its application

Zhongzhong Liu [a,b], Hanpeng Wang [a,b,*], Liang Yuan [c], Bing Zhang [a,*], Wei Wang [a,b], Zhengwei Ma [a,b], Yang Xue [a,b], Yong Li [c]

[a] Research Centre of Geotechnical and Structural Engineering, Shandong University, Jinan 250061, China
[b] School of Qilu Transportation, Shandong University, Jinan, Shandong 250061, China
[c] Faculty of Safety Engineering, China University of Mining and Technology, Xuzhou 221116, China

ARTICLE INFO

Article history:
Received 26 April 2019
Received in revised form 8 August 2019
Accepted 8 September 2019
Available online 12 September 2019

Keywords:
Geotechnical mechanics
Standard cylindrical specimens
Circumferential deformation
Test method
System development

ABSTRACT

A new test method and system was proposed for circumferential deformation of cylindrical standard specimens. It has clear testing principle, exquisite structure, low cost and high accuracy. Its high reliability and repeatability were verified by comparing with MTS chain extensometer and close-range photogrammetry, and the error between it and MTS method is less than 0.22% in the Poisson's ratio test. This system can be used in gas-solid coupling, triaxial loading and other loading environments and it is applied to the coal adsorption degradation test under different adsorption pressures in this paper. The deformation pattern and the instability failure of coal during loading were obtained, and the influence of the adsorption pressure on volume expansion, coal strength and fracture development was analysed. This system is important to improve the rock mechanics test method and to upgrade the old testing machine.

1. Introduction

Rock mechanics laboratory test, as the main analysis and monitoring method to study the complex natural structure and physical and mechanical properties of rocks, plays a decisive role in the design and construction of rock engineering. Deformation monitoring of cylindrical standard specimens is one of the basic physical monitoring parameters in rock mechanics laboratory tests, and it is very important to study the mechanical properties of rocks under environmental and loading conditions

Thomas Young found that the longitudinal deformation of materials was accompanied by the circumferential deformation in the tensile and compression tests in 1807. Simeon Denis Poisson put forward the concept of the elastic constant in 1829, Poisson's ratio. Research shows that the circumferential deformation of rock samples deviates from the linear relationship between the circumferential deformation and the axial stress earlier and faster than that between the axial deformation and the axial stress under uniaxial compression [1,2]. However, further research is lacking due to the difficulty in monitoring the circumferential deformation in the elastic stage, especially in the post-peak plastic stage. At present, the measurement methods for circumferential deformation in rock mechanics tests can be divided into two categories: non-contact methods and contact methods.

Non-contact measurement methods mainly include the optical interferometry method, the photoconductive thermoplastic holography method and the digital speckle in-plane correlation method (DSCM) [3,4]. For example, Seebacher et al. obtained the Young's modulus and Poisson's ratio of the materials using the holography method [5]. Yamaguchi proposed a non-contact laser speckle strain gauge [6]. The full-field and local displacements of the two groups of concrete specimens in the bending fatigue test were obtained by DSCM [7]. The three-dimensional displacement and strain of the sandstone before and after the deformation in the three-point bending test were obtained based on the DSCM, and the initial load and subcritical crack growth length were verified [8]. However, the disadvantages of this method are that the cost of the system is high, and the accuracy is greatly affected by external factors such as light, environment, operation and so on.

* Corresponding authors at: School of Qilu Transportation, Shandong University, No. 17923, Jingshi Road, Jinan, Shandong 250061, China (H. Wang). Research Centre of Geotechnical and Structural Engineering, Shandong University, No. 17923, Jingshi Road, Jinan, Shandong 250061, China (B. Zhang).

E-mail addresses: whp@sdu.edu.cn (H. Wang), 201413178@mail.sdu.edu.cn (B. Zhang).

https://doi.org/10.1016/j.measurement.2019.107041
0263-2241/

The contact method is the mainstream method for circumferential deformation measurement, represented by the mechanical method, electrical method and extensometer method [9,10]. The mechanical method mainly uses a mechanical micrometre or LVDT sensor, which is installed on the surface of the specimen to obtain the displacement of the measuring point directly. Osorio et al. obtained the circumferential strain by arranging six LVDT sensors around the specimen [11]. However, there are some errors in expressing the circumferential deformation of the specimens by the deformation of some points. The electrical method is to paste longitudinal and transverse resistance strain gauges on the specimens, and indirectly measure the circumferential deformation by collecting micro-strains of the strain gauges. In the hydrostatic test of sandstone cores, the circumferential deformation was measured by strain gauges, and the effective stress coefficient was deduced accordingly [12]. Hsieh et al. measured both axial and circumferential strains of specimens by cross-laying strain gauges [13]. However, the measurement error of this method is large because the adhesion of strain gauges will increase the local stiffness of the specimens. Moreover, the post-peak displacement cannot be measured. Finally, the operation of this method is inconvenient, and the strain gauges are disposable. In the extensometer method, a complete set of sensors is installed on the surface of the specimen, and the strain data are acquired by secondary instruments. Aydan et al. measured the circumferential deformation of the rock in creep test using a chain extensometer, and determined the ISRM suggested method of creep characteristics of the rock [14]. The MTS (Material Testing System) had developed a method and instrument for measuring the circumferential deformation based on a chain extensometer, and this method has been widely used. For example, Huang et al. obtained the circumferential deformation of soft rock in a triaxial unloading confining pressure test and triaxial unloading creep test using an MTS chain extensometer and studied the dilatancy and failure characteristics of the soft rock [15]. Qiu et al. measured the circumferential deformation of marble pre-peak deformation using an MTS chain extensometer and proposed a new model to describe the evolution characteristics of the pre-peak unloading damage [16]. In addition, the grating sensor was also used to measure the material transverse-vertical deformation and Poisson's ratio [17,18].

At present, the three methods widely used in circumferential deformation measurements are the cantilever type, the MTS chain type and the GDS LVDT extensometer (Fig. 1).

In conclusion, remarkable results have been achieved in the development of circumferential deformation measuring system, but there are still some problems such as high cost, large volume and low accuracy. Moreover, due to the difficulty of monitoring the circumferential deformation in the elastic stage, especially in the post-peak plastic stage, there are few related studies, which need to be further strengthened. Based on the existing methods and techniques of circumferential deformation measurement, a new method and system for geotechnical cylindrical specimens is proposed based on angle measurement.

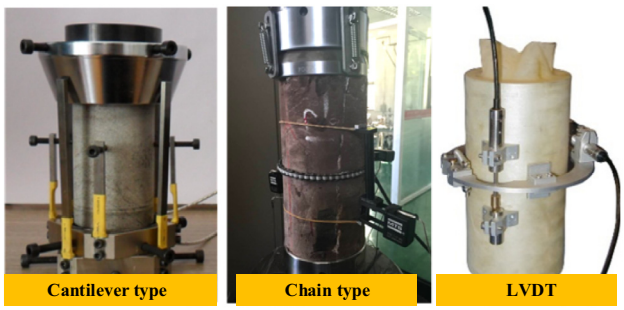

Fig. 1. Common Circumferential Deformation Testing Device.

2. System composition and testing principle and method

2.1. System composition

This system consists of a chain-type rolling belt, a holding structure (including a fixed disk, preloaded spring, fixed pointer and flexible pointer), angle sensor, DAQ data acquisition card and acquisition program (Fig. 2).

The chain type rolling belt and holding structure are all made of stainless steel. The angle sensor can be a conductive plastic potentiometer or Hall angular displacement sensor, which can output a 0–5 V voltage signal from an angle change of 0–360 degrees, and the data will be collected and recorded by acquisition system. The conductive plastic potentiometer is rated to withstand 1000 V/min in terms of its insulation voltage value. The Hall angular displacement sensor is a non-contact magnetoelectronic effect sensor and its working environment temperature is −55 °C−125 °C. Both of them can work in a high pressure gas or in hydraulic oil and can be used in a multiphase coupled loading test.

2.2. Principle and method

During the test, the chain rolling belt is wound in the middle of the standard cylindrical specimen. The fixed pointer and the flexible pointer are connected with the two ends of the chain rolling belt, which is fixed by the pre-tightening spring. The other end of the fixed pointer and the flexible pointer are respectively connected with the fixed disk and the rotating shaft of the angle sensor. When the circumferential deformation occurs, the distance between the two ends of the chain rolling belt will change, resulting in the change of the angle between the two pointers. The angle change value θ_e is record by the angle sensor and is used to calculate the circumferential deformation of the specimen. The principle is shown in Fig. 3.

Set the length of chain rolling belt as l_c, the radius of ball bearing as r, specimen radius before deformation as R, the circumferential strain as ε, and the specimen radius after deformation as $R(1+\varepsilon)$. The radius angle of the chain rolling belt after the deformation of the specimen is α, and the chord length in Fig. 3 is l_f. The length of the chain rolling belt l_c remains unchanged before and after deformation. Then, we can get Eqs. (1) and (2).

$$l_c = [R(1+\varepsilon) + r] \tag{1}$$

$$l_f = [2R(1+\varepsilon) + r] \times \sin\frac{\alpha}{2} \tag{2}$$

The chord length l_f can also be obtained from the measured angle θ_e:

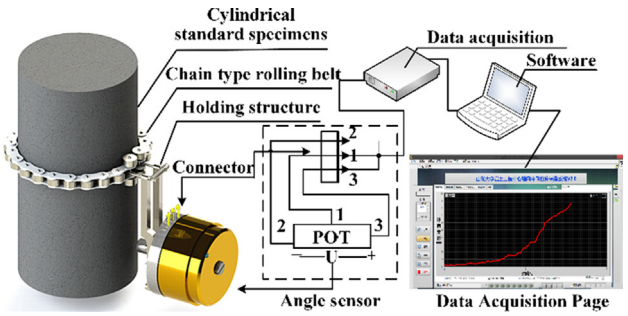

Fig. 2. The composition of circumferential deformation measurement system.

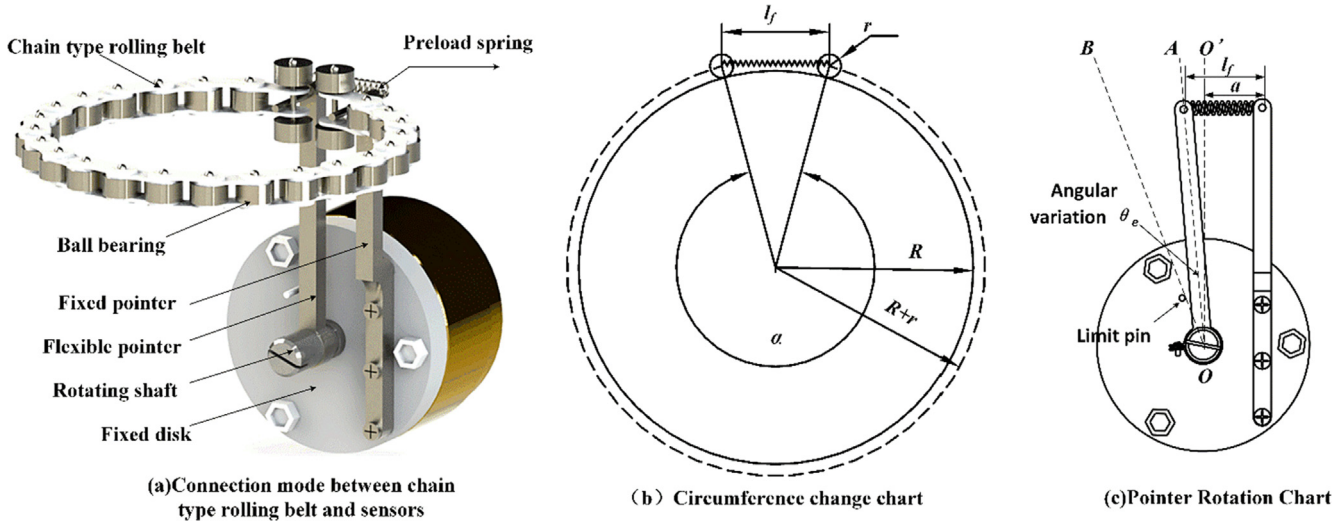

Fig. 3. Testing principle.

$$l_f = a + L\sin\theta_e \tag{3}$$

We can obtain Eq. (4) from Eqs. (1)–(3):

$$a + L\sin\theta_e = 2[R(1+\varepsilon)+r]\sin\frac{l_c}{2[R(1+\varepsilon)+r]} \tag{4}$$

Because the length l_c of the chain rolling belt, radius r of the ball bearing and radius R of the specimen are known, the circumferential strain ε of specimen can be obtained by substituting the measured angle value θ_e into Eq. (4).

The measurement range of the circumferential strain is related to the stiffness coefficient and the material quality of the pretensioned spring. The spring used in this paper is 304 stainless steel. The spring's maximum tension force is 5 N and its stiffness coefficient is 0.17 N/mm. The maximum circumferential deformation is 30 mm and it can meet the testing requirements for coal and rock mass materials except for the accelerated creep deformation test of rock salt creep materials at the later stage [19]. To prevent the device from being damaged due to excessive deformation, a limit pin is set at the appropriate position on the straight line *OB* with an angle 25 degrees from the normal. The straight line *OB* is determined by the maximum deformation of the specimen. In terms of the system test accuracy, because the resolution of the conductive plastic potentiometer is infinitely smaller in theory, the test accuracy depends on the accuracy of the DAQ data acquisition controller. The accuracy of the angle sensor and data acquisition card are both 0.1% F.S., and the angle resolution is $\Delta\theta = 0.36$ degrees, which is converted into the circumferential deformation resolution $P' = L\sin(\Delta\theta) = 0.004$ mm (L is the length of flexible pointer and $L = 39.5$ mm).

3. Main dimensions and technical advantages

3.1. Main dimensions

The main dimensions of some major components are shown in Table 1.

3.2. Technical advantages

Compared with the existing measuring instruments and methods, the circumferential deformation measuring method described in this paper has the following technical advantages.

Table 1
Main dimensions of some major components.

Items	Specification parameters
Ball bearing	Internal diameter: 3 mm, external diameter: 6 mm
Fixed pointer	Length: 52 mm, Side length of cross section: 3 mm
Flexible pointer	Length: 40 mm, Side length of cross section: 3 mm
Rotating shaft	Length: 15 mm, cross section diameter: 6 mm
Angle sensor	Thickness: 25 mm, cross section diameter: 36 mm

1) High accuracy. The strain gauge method will increase the local stiffness of specimens in the process of strain gauge pasting, and the measuring error is large and the post-peak deformation can not be measured. The method in this paper achieves high accuracy through ingenious structural design, and the measuring accuracy can reach 0.004 mm.
2) Low cost. Compared with MTS chain extensometer, this measuring system has similar measuring accuracy, but the price is only about one tenth of MTS chain extensometer.
3) Small size. The existing extensometer measuring method has a large cantilever volume and is not suitable for the test of specimens under gas-solid coupling conditions. The components of the method raised in this paper are all exquisite micro-components. The maximum space occupied by the whole system plus cylindrical specimens is about 500 cm^3, which is suitable for gas-solid coupling conditions.
4) High stability. The existing digital image method has high cost, and its accuracy is affected by light, environment, operation and other factors, so the measurement results are unstable. The method in this paper is simple to operate and clear in principle. The following verification tests show that it has very high stability.

4. Verification test and discussion

4.1. Test scheme

To verify the accuracy and feasibility of the system, uniaxial compression tests were carried out using polyurethane cylindrical standard specimens (Φ50 mm × 100 mm). The test pictures are shown in Fig. 4. The polyurethane cylindrical standard specimens are completely elastic and can be tested many times. The specimens under the same load have the same deformation. It is convenient to use other methods (MTS chain extensometer and close-range photogrammetry) for comparative analysis.

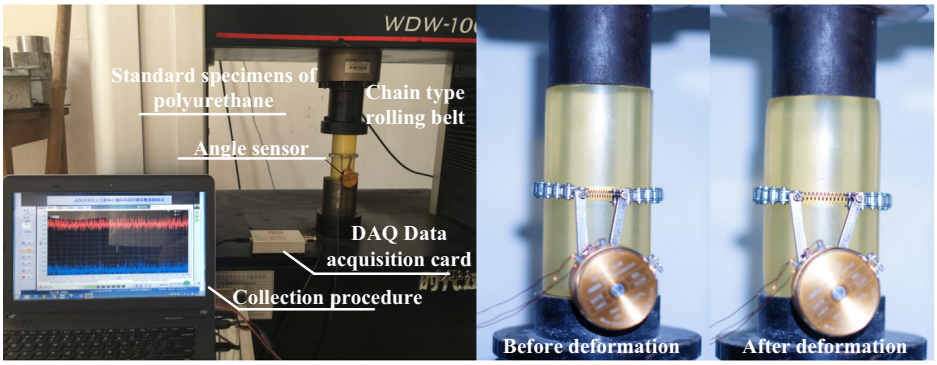

Fig. 4. Uniaxial compression test of polyurethane standard specimens.

The test loading mode is displacement loading and the loading rate is 0.3 mm/s. When the maximum loading stress reaches 2 MPa, the specimen is unloaded after 60 s, and the maximum axial displacement is 12.6 mm.

4.2. Result and discussion

The circumferential deformation of polyurethane standard specimens under different loading stresses was measured by photogrammetry. The change of the middle diameter of the specimen was identified by PHOTOINFOR in order to calculate the circumferential displacement. The test results are shown in Fig. 5. It can be seen that the degree of coincidence between the two is high, which verifies the reliability and accuracy of the system.

The Poisson's ratio of the same polyurethane specimen was tested 3 times by both the method presented in this paper and the MTS chain method. The final results are shown in Table 2. The Poisson's ratios of the polyurethane specimens measured by this method and MTS method are 0.473 and 0.472, respectively. The error is less than 0.22%, and it is consistent with the Poisson's ratios of polyurethane materials.

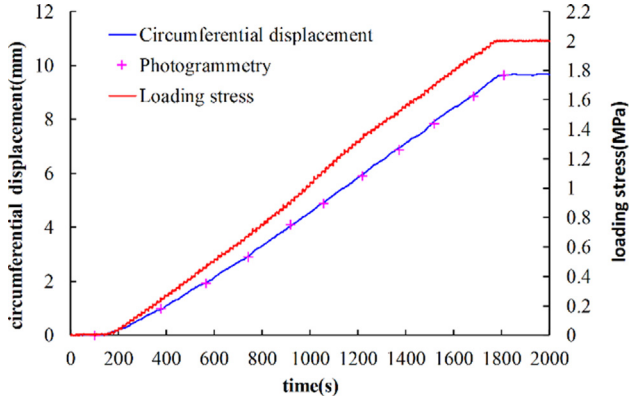

Fig. 5. Comparisons with photogrammetric measurements.

5. System application

5.1. Test material

According to the proportioning and characteristics of similar materials for gas-bearing coal developed by Wang Hanpeng et al., standard briquette samples whose uniaxial compressive strength were 1 MPa were prepared by adjusting the concentration of the cementing agent[20]. (pulverized coal with a particle size ratio of 0–1 mm: 1–3 mm = 0.76:0.24 is used as an aggregate, sodium humate solution is used as a cementing agent, and it is pressed under a press with 15 MPa.) The physical and mechanical parameters are shown in Table 3.

5.2. Test apparatus

The circumferential deformation test system and a self-developed visual constant-volume gas-solid coupling test system (VCGCTS) is used in the test[21], and its schematic diagram and photo are shown in Fig. 6. Combined with the servo press and flexible chambers, the coupling loading chamber is able to keep a constant volume and eliminate load errors due to the inner pressure change of the chamber during the pressure loading process. Moreover, equipped with visual windows, the system can achieve real-time visualization monitoring of the coal fracture development and degradation law during the whole process. It is worth mentioning here that in order to ensure the sealing performance of the lead of the circumferential deformation test system, the sealing channel of the lead is opened on the bottom board, and the lead wire is drawn from it. Enamelled wire and epoxy resin sealant were used for sealing, and the apparatus has good sealing performance after testing.

5.3. Test scheme

Briquette samples with the same strength were used and were first inflated with a specific amount of CO_2 and then inflated with He to increase the adsorption pressure. The stress-strain and deformation failure parameters were monitored in the loading process. The test parameter variables are shown in Table 4. When the coal

Table 2
Poisson's ratio of polyurethane specimen.

Test scheme	Poisson's ratio			
	1	2	3	Average value
Method of this paper	0.472	0.474	0.473	0.473
MTS chain extensometer	0.471	0.473	0.472	0.472

Table 3
Physical and mechanical parameters of standard briquette samples.

Precast strength (MPa)	Particle size distribution 0–1 mm: 1–3mm	Concentration of sodium humate (%)	Molding pressure (MPa)	Density (N cm^{-3})	Measured strength (MPa)	Elastic modulus (GPa)	Poisson's ratio	Cohesion (MPa)	Internal friction angle (°)
1	0.76:0.24	3.25	15	12.78	1.014	0.187	0.314	0.092	29

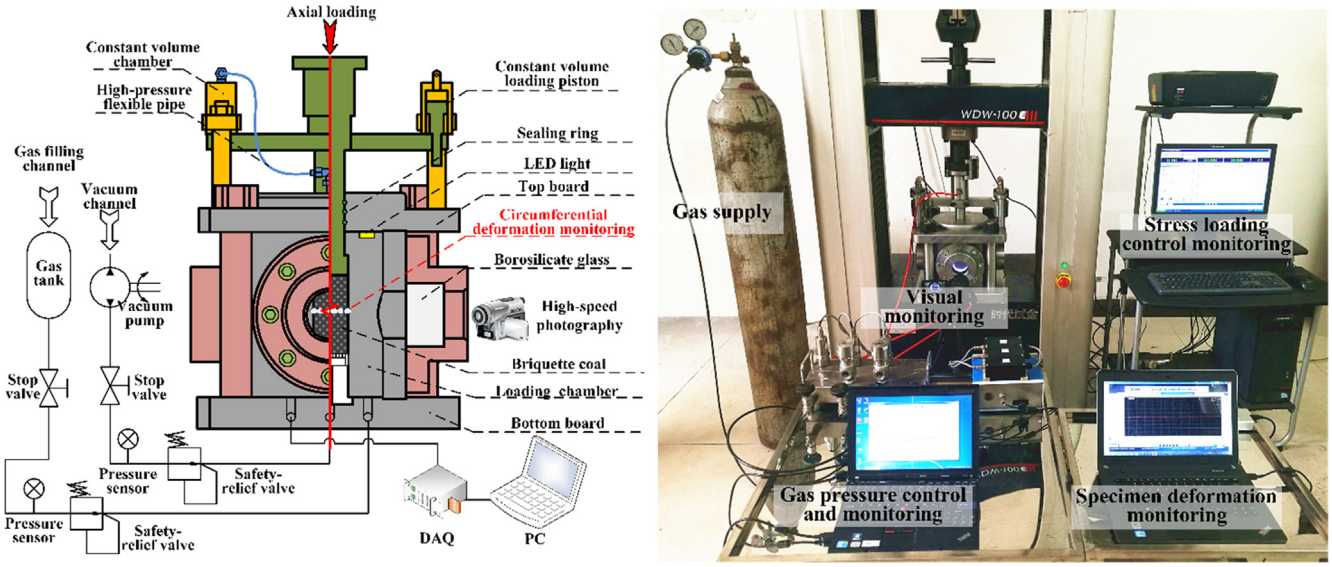

Fig. 6. The gas-solid coupling test system.

Table 4
Test key parameters.

Group number	Specimen number	Precast strength (MPa)	CO_2 pressure (MPa)	Total pressure (MPa)	Temperature (°C)	Adsorption time (h)
1	1	1.0	0.3	0.3	25	24
	2	1.0	0.3	0.6	25	24
	3	1.0	0.3	0.9	25	24
2	4	1.0	0.6	0.6	25	24
	5	1.0	0.6	0.9	25	24
	6	1.0	0.6	1.2	25	24
3	7	1.0	0.9	0.9	25	24
	8	1.0	0.9	1.2	25	24
	9	1.0	0.9	1.5	25	24

body was fully adsorbed, the specimen was loaded axially using the displacement control mode of the axial loading module, and the loading rate is 1 mm/min[22]. The coal strength, axial-circumferential deformation and fracture development were recorded and observed during the test. The stress loading path of the coal body is shown in Fig. 7.

It should be noted that under constant temperature, the gas pressure can be equivalent to the average impact force of gas molecules on the solid surface per unit area. In the same temperature-pressure environment, any gas of the same volume contains the same number of molecules, according to Avogadro's hypothesis. The volume of gas refers to the space occupied by the molecule. Usually, the average distance between the molecules of gas is approximately 10 times the diameter of the molecule. Therefore, when the number of molecules in the gas is constant, the volume of the gas mainly depends on the average distance between the

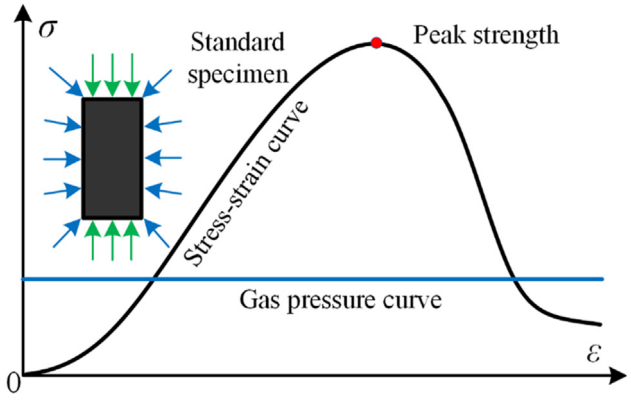

Fig. 7. Stress loading path.

Table 5
Test data.

Group number	Specimen number	Measured strength (MPa)	CO_2 pressure (MPa)	Total pressure (MPa)	Strength after adsorption (MPa)	Strengths mean after adsorption (MPa)
1	1	1.014	0.3	0.3	0.866	0.861
	2	1.014		0.6	0.862	
	3	1.014		0.9	0.857	
2	4	1.014	0.6	0.6	0.783	0.781
	5	1.014		0.9	0.779	
	6	1.014		1.2	0.78	
3	7	1.014	0.9	0.9	0.724	0.724
	8	1.014		1.5	0.719	
	9	1.014		2.1	0.73	

molecules rather than the size of the molecule itself. When the volume of the test system and the temperature is constant, the gas pressure is only related to the quantity of the gas substance according to Clapeyron equation, which is shown in Eq. (5). Whether it is CO_2 or He, the average distance between gas molecules is much larger than the diameter of the molecules, so it can be regarded as the same kind of particles. Therefore, the test method is feasible and there is no order requirement for gas inflation.

$$PV = nRT \tag{5}$$

where, P is the gas pressure, V is the gas volume, n is the amount of substance, T is the absolute temperature, and R is the gas constant.

5.4. Results

The experimental data obtained in the test is shown in Table 5. The full stress-strain curve and volume strain curve of the coal body are shown in Fig. 8 and Fig. 9. The characteristics of coal fracture development during the loading process were obtained by a high-speed monitoring camera (Fig. 10). Each group of tests was designated by "CO_2 pressure – total pressure". For example, "0.3–0.6" represented that the sample was first inflated by 0.3 MPa of CO_2, then inflated by 0.3 MPa of He, and the final adsorption pressure was 0.6 MPa.

5.5. Discussion

From the stress-strain and volume-strain curves, the following can be concluded. 1) As an inert gas, He has no adsorption on coal. 2) The strength reduction in coal after adsorption is only related to the unit volume content of the adsorptive gases but not to the total pressure of the mixed gases. 3) The higher the carbon dioxide pressure is, the smaller the slope of stress-strain curve is at the initial loading stage. 4) With the increase in the content of the adsorptive gas, the node for the volume strain of coal advances continuously from negative to positive, and the coal body reaches peak strength and enters the failure stage earlier.

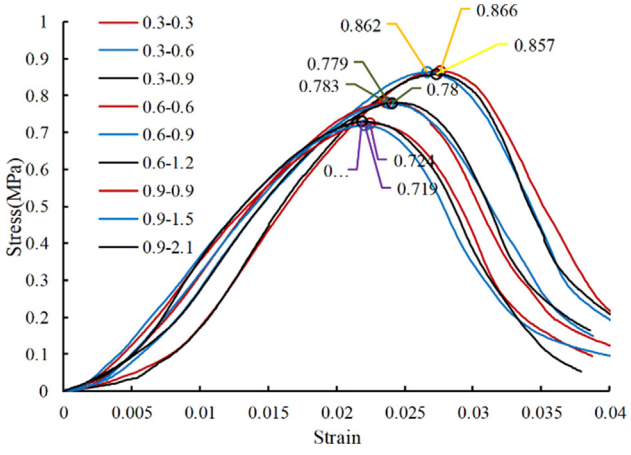

Fig. 8. Stress-strain contrast curve.

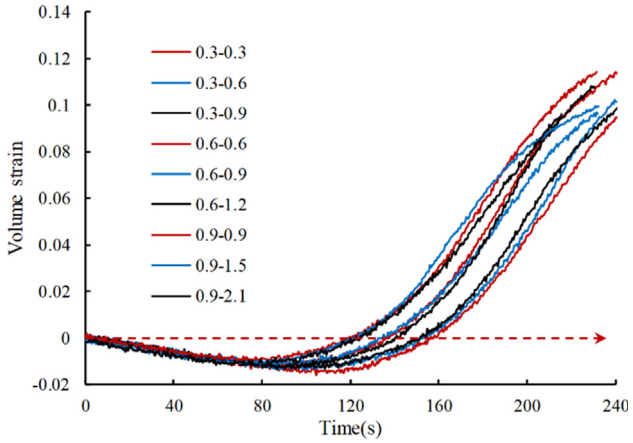

Fig. 9. Volume strain contrast curve.

It can be seen from Fig. 10 that with the increase in the content of adsorptive gas, the coal body cracks at the same stress stage develop more abundantly and the crack lines become more complex. When the pressure of CO_2 is 0.3 MPa, the coal body mainly develops along 1–2 macro-cracks, and ultimately destabilizes. When the pressure of CO_2 is 0.9 MPa, the main cracks of coal body are no longer obvious, and a large number of net cracks are produced. The destabilizing failure mode is also changed from typical shear or tensile failure to a "fish scale" expansion and fragmentation mode.

6. Conclusions

1) A new method and system for testing the circumferential deformation of geotechnical cylindrical specimens based on angle measurement was developed. It can be used to measure the Poisson's ratio of standard cylindrical specimens and the circumferential deformation in post-peak mechanical behaviour in geotechnical tests. It can be used in conventional triaxial and gas-solid coupling tests.
2) The reliability and accuracy of the test system are verified by an MTS chain extensometer and through close-range photogrammetry using polyurethane cylindrical standard specimens. It was applied to the coal adsorption deformation test,

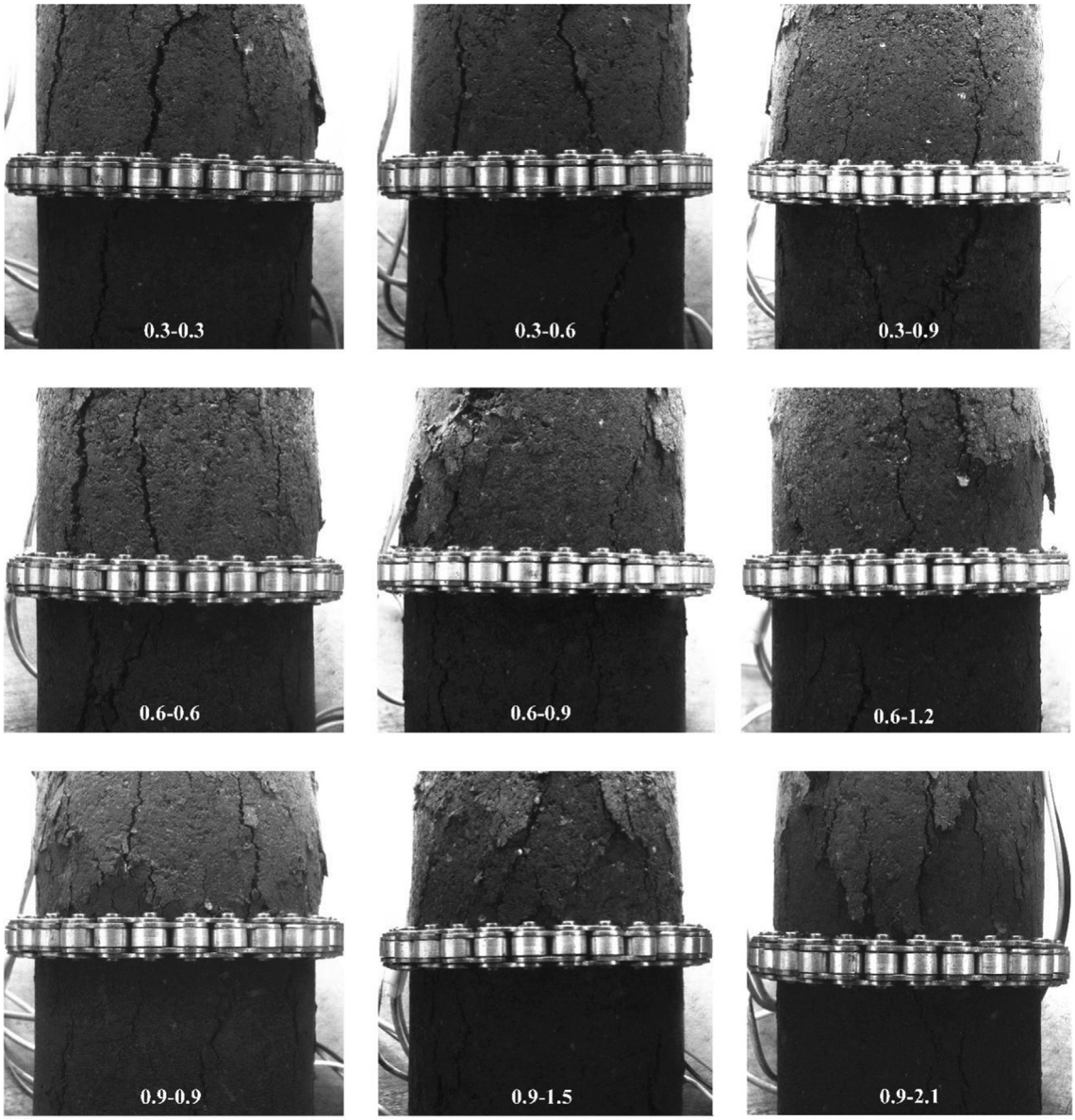

Fig. 10. Monitoring of coal circumferential deformation under different adsorption pressure.

and the circumferential deformation and total stress-strain curves of coal during gas-solid coupling loading were obtained. Moreover, the law describing the influence of the gas adsorption quantity on the volume strain and degradation rate of the coal body was obtained.

3) The principle of this test method is clear, and a modular design concept is adopted in the test system. It can achieve rapid synchronous acquisition with the axial LVDT displacement meter. It is of great significance to enrich the rock mechanics test method and to upgrade the old testing machine.

Declaration of Competing Interest

The authors declare that they have no known competing financial interests or personal relationships that could have appeared to influence the work reported in this paper.

Acknowledgements

This work was financially supported by National Natural Science Foundation of China (51427804), Natural Science Foundation of Shandong Province (2019GSF111036, ZR2017MEE023).

References

[1] Kiyama Fujii, Kodama Ishijima, Circumferential strain behavior during creep tests of brittle rocks International, J. Rock Mech. Mining Sci. 36 (1999) 323–337.
[2] Z. Wang, Z. Zong, L. Qiao, W. Li, Transversely isotropic creep model for rocks, Int. J. Geomech. 18 (2018).
[3] M. Angelidi, A.P. Vassilopoulos, T. Keller, Displacement rate and structural effects on Poisson ratio of a ductile structural adhesive in tension and compression, Int. J. Adhes. Adhes. 78 (2017) 13–22.
[4] H. Zhu, L. Hu, Displacement measurement using digital speckle multi-frequency harmonic wave correlation method, Measurement 89 (2016) 7–12.
[5] S. Seebacher, W. Osten, T. Baumbach, W. Jüptner, The determination of material parameters of microcomponents using digital holography, Opt. Lasers Eng. 36 (2001) 103–126.

[6] I. Yamaguchi, A laser-speckle strain gauge, J. Phys. E: Sci. Instrum. 14 (2000) 1270.
[7] LiPing Guo, W. Sun, XiaoYuan He, ZhenBin Xu, Application of DSCM in prediction of potential fatigue crack path on concrete surface, Eng. Fract. Mech. 75 (2008) 643–651.
[8] J. Zuo, Y. Li, X. Zhang, Z. Zhao, T. Wang, The effects of thermal treatments on the subcritical crack growth of Pingdingshan sandstone at elevated high temperatures, Rock Mech. Rock Eng. (2018) 1–16.
[9] K.T. Nihei, L.B. Hilbert, N.G.W. Cook, S. Nakagawa, L.R. Myer, Frictional effects on the volumetric strain of sandstone, Int. J. Rock Mech. Min. 37 (2000) 121–132.
[10] A. Fakhimi, E. Alavi Gharahbagh, Discrete element analysis of the effect of pore size and pore distribution on the mechanical behavior of rock, Int. J. Rock Mech. Min. 48 (2011) 77–85.
[11] Edison Osorio, M. Jesus Bairan, R. Antonio Mari, Lateral behavior of concrete under uniaxial compressive cyclic loading, Mater. Struct. 46 (2013) 709–724.
[12] X. Ma, Volumetric deformation, ultrasonic velocities and effective stress coefficients of st peter sandstone during poroelastic stress changes, Rock Mech. Rock Eng. (2019).
[13] A. Hsieh, A.V. Dyskin, P. Dight, The increase in Young's modulus of rocks under uniaxial compression, Int. J Rock Mech. Min. 70 (2014) 425–434.
[14] Ö. Aydan, T. Ito, U. Özbay, M. Kwasniewski, K. Shariar, T. Okuno, A. Özgenoğlu, D.F. Malan, T. Okada, ISRM suggested methods for determining the creep characteristics of rock, Rock Mech. Rock Eng. 47 (2014) 275–290.
[15] X. Huang, Q. Liu, B. Liu, X. Liu, Y. Pan, J. Liu, Experimental study on the dilatancy and fracturing behavior of soft rock under unloading conditions, Int. J. Civil Eng. 15 (2017) 1–28.
[16] S.L. Qiu, X.T. Feng, J.Q. Xiao, C.Q. Zhang, An experimental study on the pre-peak unloading damage evolution of marble, Rock Mech. Rock Eng. 47 (2014) 401–419.
[17] C. Yilmaz, Monitoring Poisson's ratio of glass fiber reinforced composites as damage index using biaxial Fiber Bragg Grating sensors, Polym. Test. 53 (2016) 98–107.
[18] W.V. Paepegem, I.D. Baere, E. Lamkanfi, J. Degrieck, Monitoring quasi-static and cyclic fatigue damage in fibre-reinforced plastics by Poisson's ratio evolution, Int. J. Fatigue 32 (2010) 184–196.
[19] Q.B. Zhang, J. Zhao, A review of dynamic experimental techniques and mechanical behaviour of rock materials, Rock Mech. Rock Eng. 47 (2014) 1411–1478.
[20] H.P. Wang, Q.H. Zhang, L. Yuan, J.H. Xue, L.I. Qing-Chuan, W. Zhou, L.I. Jian-Ming, B. Zhang, Development of a similar material for methane-bearing coal and its application to outburst experiment, Rock Soil Mech. 36 (2015) 1676–1682.
[21] Q.C. Li, H.P. Wang, S.C. Li, L. Yuan, J.H. Xue, B.L. Chen, B. Ren, Development and application of visual constant volume gas-solid coupling test system, J. China Univ. Mining Technol. 47 (2018).
[22] N.S.C.G. China, Standard for Test Method of Engineering Rock Mass, GB/T50266—99, Beijing: China Planning Publishing House, 1999, pp. 15–16.